*Progress In Electromagnetics Research, Vol. 144, 193–200, 2014*

# A Multi-Evanescent-Mode Coaxial Cavity Resonator

**Jin-Song Zhan[1, *], Shi-Wei Dong[2], Li-Ming Gong[2], Shao-Feng Dong[1], Xiao-Long Chen[1], and Jia-Li Wang[1]**

**Abstract**—This paper presents a novel miniaturized multi-evanescent-mode resonator. The resonator is achieved with a coaxial cavity. This coaxial cavity essentially has a direct short connection at one end and is connected with several lumped capacitances at the other end. The key technology of the resonator is the usage of multiple evanescent-modes of TM (transverse magnetic wave) modes. Due to the combined effects of the evanescent mode and multiple modes, the size of the resonator is greatly reduced. In this paper, the theory of resonator is discussed in detail. To verify the correctness of operation, the resonator is used in experimental measurements conducted to realize a third-order band-pass filter based on SIW (substrate-integrated waveguide) technology. The measured results are found to agree with the theoretical values.

## 1. INTRODUCTION

In recent years, the rapid growth of wireless communication systems has caused the extensive use of high performance and compact microwave filters, duplexers and matching circuits with low insertion loss. The literature includes reports on various types of miniaturized techniques, such as evanescent-modes [1–8], dual-modes [9–11], SIW (substrate integrated waveguide) [12–14], SIR (stepped impedance resonators) [15, 16]. Unfortunately, most studies focus on the realization of components at L-band or higher. Especially, in the frequency range of 100 MHz to 1 GHz, it is still difficult to reduce the size of the RF components appreciably with any one of the miniaturized technologies mentioned above. As a result, some inexpensive miniaturized components will be composed of lumped capacitances and inductances, but generally suffer from high insertion losses due to low quality factor of the lumped inductance.

In this paper, a novel miniaturized resonator is proposed for the ultra-high frequency (UHF) band. The main principle of the resonator is that it works at multiple evanescent modes. It consists of a coaxial cavity and several lumped capacitances. This resonator is very different from the evanescent-mode resonator which uses rectangular or circular waveguides [1–8]. Utilizing the SIW technology, this novel miniaturized resonator could be realized conveniently in a PCB (Printed Circuit Board) or LTCC (Low Temperature Co-fired ceramic) [17–19]. By adjusting the dimensions of coaxial cavity or the value of lumped capacitance, the resonance frequency can be changed over a wide range. It is easy to obtain a high $Q$ factor of value higher than 400 at a frequency between 100 MHz and 1 GHz. Due to the combined effects of the evanescent-modes and multi-modes, use of this resonator greatly reduces the size of the RF components.

The organization of the remaining paper is as follows. In Section 2, the theoretical solutions of the evanescent-mode multi-mode resonator are presented. The experimental measurements and applications of the multi-evanescent-mode resonator are presented in Section 3. The manufacturing techniques for third-order band-pass filter based on SIW are given. Finally, the conclusions of this study are summarized in Section 4.

*Received 29 November 2013, Accepted 9 January 2014, Scheduled 21 January 2014*

* Corresponding author: Jin-Song Zhan (327395709@qq.com).

[1] School of Mechano-Electronic Engineering, Xidian University, Xi'an 710071, China. [2] Science and Technology on Space Microwave Laboratory, CAST (Xi'an), Xi'an 710100, China.

## 2. THEORY ANALYSIS

The multi-evanescent-modes resonator is shown in Fig. 1. The dimensions of external diameter, internal diameter and length of coaxial cavity are $a$, $b$ and $h$, respectively. The coaxial cavity is direct short at one end, and connects with several lumped capacitances at the other end. It will be established later that the coaxial cavity can be treated as an inductance when working at proper evanescent modes. As a result, a resonator may be realized when the coaxial cavity is connected to several capacitances. The capacitances should be mounted at a position where electric field has maximum value. Apparently, the quantities and the positions of capacitances are determined by the electrical polarization modes and not limited to the case shown in Fig. 1. The relative dielectric constant and relative permeability in the coaxial cavity are $\varepsilon_r$ and $\mu_r$ respectively. In the proposed design, the dielectric of FR4 is chosen. The relative dielectric constant is 4.4 and the dielectric loss tangent is 0.02.

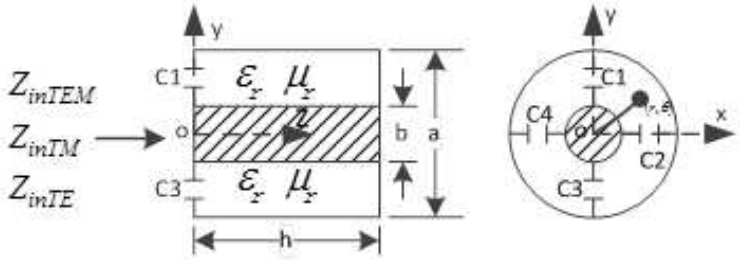


**Figure 1.** The structure of multi-evanescent- mode resonator.

According to the Maxwell's equations, the electromagnetic modes of TEM (transverse electromagnetic wave), TE (transverse electric wave) and TM (transverse magnetic wave) may be excited in the coaxial cavity. The resonance frequencies are closely related to the electromagnetic modes and the lumped capacitances.

For the TEM mode, the equivalent input impedance $Z_{in\mathrm{TEM}}$ of the coaxial cavity is given by

$$Z_{in\mathrm{TEM}} = j\frac{60}{\sqrt{\varepsilon_r}}\ln\left(\frac{a}{b}\right)\tan\left(\frac{2\pi\sqrt{\varepsilon_r}f_{0\mathrm{TEM}}}{c}h\right) \tag{1}$$

In formula (1), $c$ is the velocity of light in vacuum. The resonance frequency $f_{0\mathrm{TEM}}$ can be obtained from Equation (2).

$$-Z_{in\mathrm{TEM}} = \frac{1}{j\omega_{\mathrm{TEM}}\sum\limits_{i=1}^{n} C_i} \tag{2}$$

where $n$ is the number of capacitances. In theory, the TEM resonator can be realized despite of $\omega_{\mathrm{TEM}}$. In this paper, $h$, which is the height of PCB, will be far less than 1/4 wavelength in the UHF band. In this case, it is difficult to realize the excitation at the input/output (I/O) and the coupling between the resonators. As a result, in this type of resonators, the TEM energy is weak and can be neglected.

For the TE modes, mathematically, the electromagnetic field in the coaxial cavity can be derived from the longitudinal magnetic field $H_{z\mathrm{TE}}$[20].

$$\begin{aligned} &H_{z\mathrm{TE}} = \left[A_1 J_{m\mathrm{TE}}\left(k_{c\mathrm{TE}}r\right) + A_2 Y_{m\mathrm{TE}}\left(k_{c\mathrm{TE}}r\right)\right]\cos\left(m\theta\right)e^{-jk_{z\mathrm{TE}}z} \\ &E_{z\mathrm{TE}} = 0 \\ &k = 2\pi f\sqrt{\varepsilon_0\varepsilon_r\mu_0\mu_r} \quad \text{and} \quad k_{z\mathrm{TE}} = \sqrt{k^2 - k_{c\mathrm{TE}}^2} \end{aligned} \tag{3}$$

In the above equations, $\varepsilon_0$ is the dielectric constant, and $\mu_0$ is the permeability in vacuum. $J_{m\mathrm{TE}}(k_{c\mathrm{TE}}r)$ and $Y_{m\mathrm{TE}}(k_{c\mathrm{TE}}r)$ are Bessel function and Neumann function respectively. $A_1$ and $A_2$ are unknown variables. They are determined by an external excitation. $m$ is natural number and

related to the different electromagnetic modes. $k_{c\mathrm{TE}}$ is the cutoff wavenumber for TE modes. It can be obtained by solving Equation (4).

$$\frac{J'_m(k_{c\mathrm{TE}}a)}{J'_m(k_{c\mathrm{TE}}b)} = \frac{Y'_m(k_{c\mathrm{TE}}a)}{Y'_m(k_{c\mathrm{TE}}b)} \tag{4}$$

Utilizing $H_{z\mathrm{TE}}$, the other electromagnetic field components can be obtained as follows [20]:

$$\begin{aligned} E_{r\mathrm{TE}} &= \frac{-j}{k_{c\mathrm{TE}}^2}\frac{\omega\mu}{r}\frac{\partial H_{z\mathrm{TE}}}{\partial\theta} \quad & E_{\theta\mathrm{TE}} &= \frac{j}{k_{c\mathrm{TE}}^2}\omega\mu\frac{\partial H_{z\mathrm{TE}}}{\partial r} \\ H_{r\mathrm{TE}} &= \frac{-j}{k_{c\mathrm{TE}}^2}\beta\frac{\partial H_{z\mathrm{TE}}}{\partial r} \quad & H_{\theta\mathrm{TE}} &= \frac{j}{k_{c\mathrm{TE}}^2}\frac{\beta}{r}\frac{\partial H_{z\mathrm{TE}}}{\partial\theta} \end{aligned} \tag{5}$$

In order to obtain the resonance frequency for TE modes, the equivalent input impedance $Z_{in\mathrm{TE}}$ should be determined. At the position $z = 0$, the equivalent incident voltage $u^+$ is $\int_{b/2}^{a/2} E_{r\mathrm{TE}}dr\,|_{\theta=0}$, and the equivalent incident current $i^+$ is $\int_0^{\phi} H_{\theta\mathrm{TE}}d\theta\,\big|_{r=b/2}$. The upper limit of integral $\phi$ is determined by the parameter $m$ and it is given by $2\pi/(m+1)$. The equivalent input voltage $u$ is the summation of the incident and reflected voltages. The coaxial cavity is direct short at the position $z = h$. Therefore, the equivalent input voltage $u$ can be written as $u^+(1 - e^{-2k_{z\mathrm{TE}}h})$. Similarity, the equivalent input current $i$ can be expressed as $i^+(1 + e^{-2k_{z\mathrm{TE}}h})$. The equivalent input impedance $Z_{in\mathrm{TE}}$ is given by

$$Z_{in\mathrm{TE}} = \frac{u}{i} = \frac{u^+}{i^+}\tanh(k_{z\mathrm{TE}}h) \tag{6}$$

According to formulas (3), (4), (5) and (6), $Z_{in\mathrm{TE}}$ is a capacitive reactance for TE evanescent modes. Under these conditions, the resonator cannot be implemented unless the coaxial cavity connects with several lumped inductances at the other end.

On a basis similar to abovethe electromagnetic field in the coaxial cavity can be derived from the longitudinal electric field $E_z$ for the TM modes [20].

$$\begin{aligned} E_{z\mathrm{TM}} &= [A_1 J_{m\mathrm{TM}}(k_{c\mathrm{TM}}r) + A_2 Y_{m\mathrm{TM}}(k_{c\mathrm{TM}}r)]\cos(m\theta)\,e^{-jk_{z\mathrm{TM}}z} \\ H_{z\mathrm{TM}} &= 0 \\ k_{z\mathrm{TM}} &= \sqrt{k^2 - k_{c\mathrm{TM}}^2} \end{aligned} \tag{7}$$

where, $k_{c\mathrm{TM}}$ is the cutoff wavenumber for TM modes. It can be obtained by solving Equation (8).

$$\frac{J_m(k_{c\mathrm{TM}}a)}{J_m(k_{c\mathrm{TM}}b)} = \frac{Y_m(k_{c\mathrm{TM}}a)}{Y_m(k_{c\mathrm{TM}}b)} \tag{8}$$

The values of $a = 20\,\mathrm{mm}$ and $b = 5\,\mathrm{mm}$ are assumed in this paper. From the numerical solution, the values of partial $k_{c\mathrm{TM}}$ and corresponding cutoff frequencies are obtained which are as follows:

$$\begin{aligned} k_{c\mathrm{TM}01} &= 403.890, \quad & f_{c\mathrm{TM}01} &= 9.1873\,\mathrm{GHz} \\ k_{c\mathrm{TM}11} &= 440.159, \quad & f_{c\mathrm{TM}11} &= 10.012\,\mathrm{GHz} \\ k_{c\mathrm{TM}21} &= 529.635, \quad & f_{c\mathrm{TM}21} &= 12.047\,\mathrm{GHz} \end{aligned}$$

It can be seen that all the TM modes are evanescent modes at UHF band. In the formula (7), for simplicity, $A_1$ is assumed as 1. Obviously, the assumption will not influence the equivalent impedance $Z_{in\mathrm{TM}}$ of the coaxial cavity. The ratio of $A_2$ and $A_1$ is given by

$$\frac{A_2}{A_1} = \frac{J_{m\mathrm{TM}}(k_{c\mathrm{TM}}a)}{Y_{m\mathrm{TM}}(k_{c\mathrm{TM}}a)} \tag{9}$$

Basing on the $E_{z\mathrm{TM}}$, the other electromagnetic field components as shown below can be obtained.

$$\begin{aligned} E_{r\mathrm{TM}} &= \frac{-j}{k_{c\mathrm{TM}}^2}\beta\frac{\partial E_{z\mathrm{TM}}}{\partial r} \quad & E_{\theta\mathrm{TM}} &= \frac{-j}{k_{c\mathrm{TM}}^2}\frac{\beta}{r}\frac{\partial E_{z\mathrm{TM}}}{\partial\theta} \\ H_{r\mathrm{TM}} &= \frac{j}{k_{c\mathrm{TM}}^2}\frac{\omega\varepsilon}{r}\frac{\partial E_{z\mathrm{TM}}}{\partial\theta} \quad & H_{\theta\mathrm{TM}} &= \frac{-j}{k_{c\mathrm{TM}}^2}\omega\varepsilon\frac{\partial E_{z\mathrm{TM}}}{\partial r} \end{aligned} \tag{10}$$

The equivalent input impedance $Z_{in\mathrm{TM}}$ can be obtained with a method similar to that used for $Z_{in\mathrm{TE}}$. It should be emphasized that $Z_{in\mathrm{TM}}$ is an inductive reactance for TM evanescent modes. It means that the TM evanescent modes resonator can be realized when some capacitors are connected with the coaxial cavity according to the distribution of electric field. The capacitors should be assembled at the position where the electric field strength is maximum as shown in Fig. 2. The number of capacitors is related to the parameter $m$. It should be $2m$. In this paper, the TM01, TM11 and TM21 modes will be employed to realize a third evanescent-mode band-pass filter. It can be found that the maximum value of $m$ is 2, which means, four capacitors are necessary. Defining $\omega_{\mathrm{TM01}}$ as the resonant frequency for TM01 evanescent mode, it can be obtained when the capacitive reactance and the equivalent input impedance $Z_{in\mathrm{TEM01}}$ are equal. Assuming that the capacitance values of $C1$, $C2$, $C3$ and $C4$ all equal to $C_p$, the relation of impedance can be expressed as

$$Z_{in\mathrm{TM01}} = \frac{-1}{j\omega_{\mathrm{TM01}}4C_P} \tag{11}$$

For TM11 and TM21 evanescent modes, the magnetic walls should be considered for determining the resonant frequencies $\omega_{\mathrm{TM11}}$ and $\omega_{\mathrm{TM21}}$. The magnetics walls are located where the electric field strength equals zero, as shown in Fig. 2, On this basis, following relationships are obtained.

$$Z_{in\mathrm{TM11}} = \frac{-1}{j\omega_{\mathrm{TM11}}C_P} \tag{12}$$

$$Z_{in\mathrm{TM21}} = \frac{-1}{j\omega_{\mathrm{TM21}}C_P} \tag{13}$$

So far, the resonant frequencies are determined for the multi-evanescent-mode resonator. For the value of length $h$ equal to 2.5 mm, the dependence of resonant frequencies on $C_p$ is shown in Fig. 2.

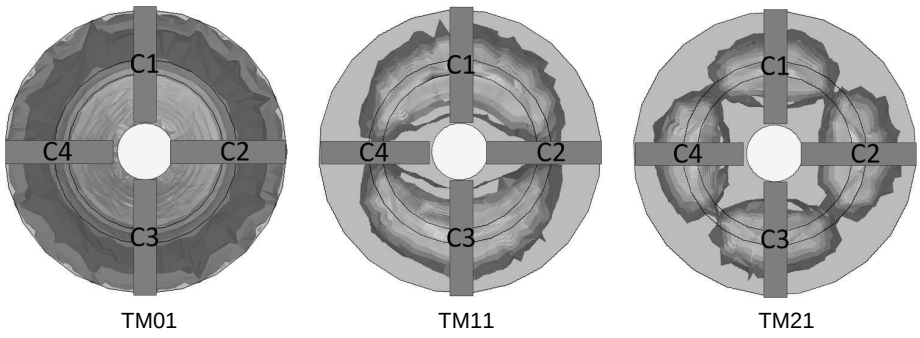


**Figure 2.** The electric field in coaxial cavity and the position of capacitors.

In fact, if six capacitors are employed, the TM31 evanescent-mode resonator can be implemented. But the corresponding resonant frequency $\omega_{\mathrm{TM31}}$ deviates appreciably from the center frequency $0.5(\omega_{\mathrm{TM21}} + \omega_{\mathrm{TM01}})$. For example, $\omega_{\mathrm{TM31}}$ equals to 2pi*1.168*$10^9$ rad/s when $C_p = 47$ pF. Obviously, $\omega_{\mathrm{TM31}}$ is difficult to be implemented for a band-pass filter with the resonant frequencies $\omega_{\mathrm{TM01}}$, $\omega_{\mathrm{TM11}}$ and $\omega_{\mathrm{TM21}}$. Generally the same is the case with other TM evanescent modes. As a result, only $\omega_{\mathrm{TM01}}$, $\omega_{\mathrm{TM11}}$ and $\omega_{\mathrm{TM21}}$ are utilized in this study.

Referring to Fig. 3, it can be noticed that the frequency difference $\omega_{\mathrm{TM21}} - \omega_{\mathrm{TM01}}$ determines the bandwidth of a band-pass filter. According to Equations (7)–(13), the frequency difference can be regulated by adjusting the dimensions of external and internal diameters, $a$ and $b$ respectively. Fixing the dimension of either $a$ or $b$, and increasing the length of the other causes the frequency difference to decrease. Fig. 4 illustrates a case in which a is increased while keeping $b$ fixed at 2 mm. Under this condition, it is unavoidable to influence the corresponding resonant frequency. This problem can be solved by reducing the $C_p$ of the capacitances values appropriately. Off course, the frequency difference changes slightly due to tuning $C_p$. It could be found in Fig. 3.

The quality factor is an important characteristic for a resonator. As widely known, the insertion loss and out band rejection are influenced strongly by the quality factor in design of a filter or duplex. For the third evanescent-mode resonator discussed in this paper, the quality factors can be extracted from full-wave simulations. The surface of coaxial cavity is copper. Fig. 5 shows that tuning the capacitance value $C_p$, changes the quality factor. The quality factor can be seen as more than 400 even when the minimum value for TM21 mode is obtained. The quality factors for another evanescent mode also can be obtained by the full-wave simulations. It can be found that the values are all less than 150. Mainly for this reason only third evanescent modes are utilized in this study.

In practice, to get an optimum flatness in pass band, it is desirable to set $\omega_{\mathrm{TM11}}$ to $0.5\,(\omega_{\mathrm{TM01}} + \omega_{\mathrm{TM21}})$. According the electric field distribution shown in Fig. 2, the capacitors $C2$ and $C4$ have no effect on TM11 evanescent mode except for the TM01 and TM21 modes. Therefore, the values of $C2$ and $C4$ can be changed to adjust the resonant frequency $\omega_{\mathrm{TM01}}$ and $\omega_{\mathrm{TM21}}$. The smaller

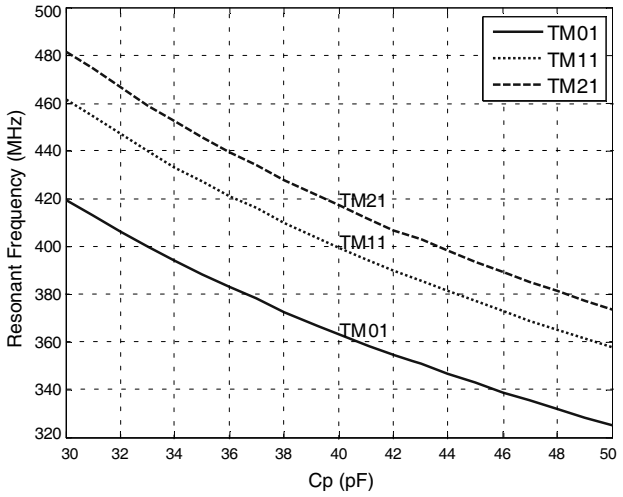


**Figure 3.** The dependence of resonant frequencies on $C_p$.

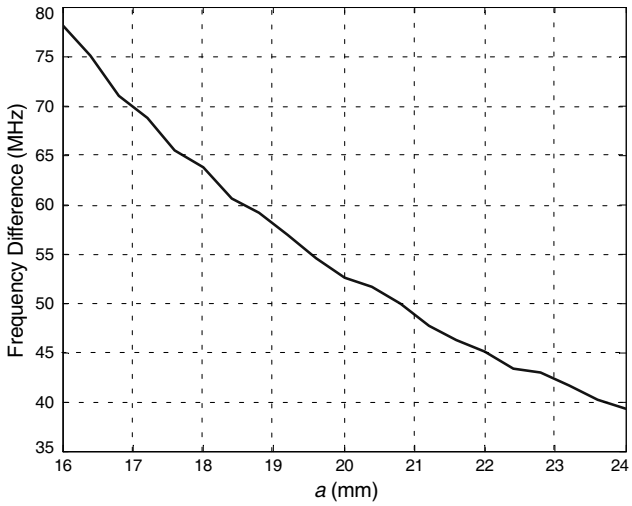


**Figure 4.** The influence of cavity dimensions on frequency difference ($a$ increasing with $b$ fixed at 2 mm).

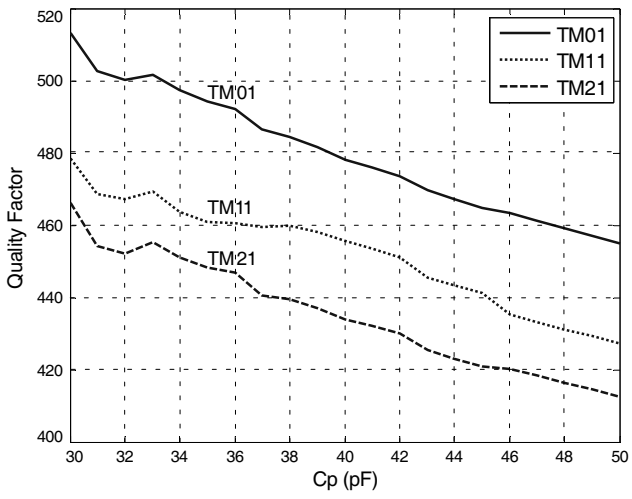


**Figure 5.** The relationship between the quality factors and $C_p$.

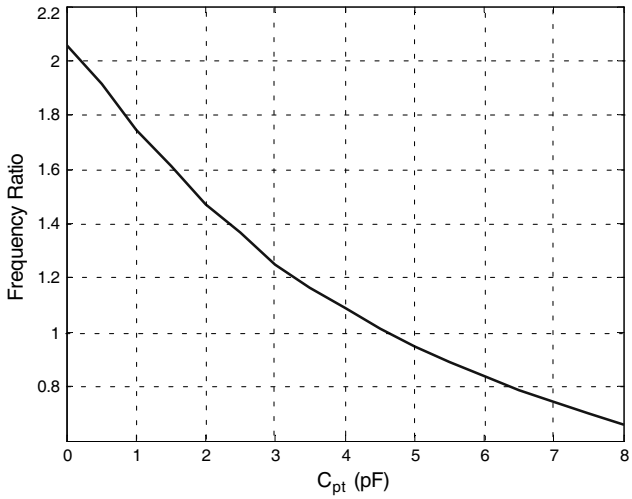


**Figure 6.** Variation of the $freq\_ratio$ with $C_{pt}$.

the values of $C2$ and $C4$ the higher are $\omega_{\mathrm{TM01}}$ and $\omega_{\mathrm{TM21}}$. By examining Fig. 3, it can be seen that $\omega_{\mathrm{TM11}}$ can be made the center frequency by increasing $\omega_{\mathrm{TM01}}$ and $\omega_{\mathrm{TM21}}$. A frequency ratio is defined by Equation (14)

$$freq\_ratio = \frac{\omega_{\mathrm{TM01}} - \omega_{\mathrm{TM11}}}{\omega_{\mathrm{TM11}} - \omega_{\mathrm{TM21}}} \tag{14}$$

Obviously, if $freq\_ratio = 1$ the resonant frequencies obtain an optimum distribution for a band-pass filter. For example, when $C1 = C3 = 42\,\mathrm{pF}$ and $C2 = C4 = 42\,\mathrm{pF} - C_{pt}$, the $freq\_ratio$ can be also extracted from full-wave simulations, as shown in Fig. 6. It can be found from the figure that $freq\_ratio$ equals 1, when $C_{pt} = 4.6\,\mathrm{pF}$.

## 3. APPLICATION AND MEASUREMENTS

To verify the analysis mentioned before, a third-order band-pass filter is designed based on one multi-evanescent-mode coaxial cavity. The SIW technology is utilized. The results have indicated that the resonant cavity can be implemented conveniently in a PCB. The model of band-pass filter is shown in Fig. 7. The relative dielectric constant is $\varepsilon_r$ and the thickness of PCB is $h$. The metal vias are used to realize the outer and inner conductors for the coaxial cavity. The dimensions of external and internal diameters of the cavity are $a$ and $b$ respectively. Two exciting ports are distributed symmetrically. The end of exciting probe is connected to the outer conductor by a transmission line. The symbol $FL$ represents the distance between the axis of the exciting port and the coaxial cavity. $C_P$ and $C_P$-$C_T$ are the values of the capacitors as shown in the figure. All the parameters are shown in Table 1. The

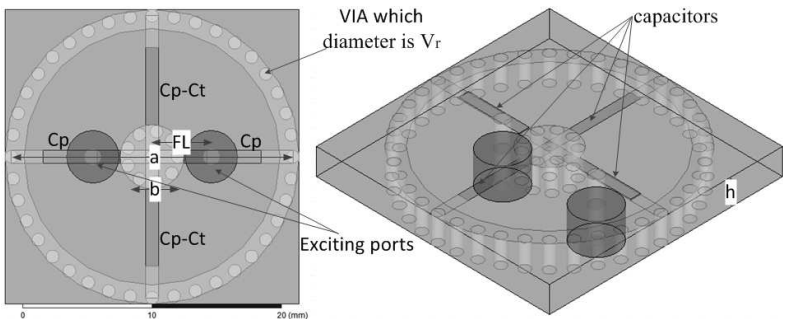


**Figure 7.** The third-evanescent-modes band-pass filter based on SIW technology.

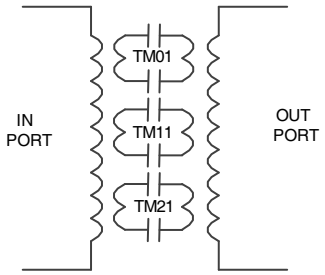


**Figure 8.** The equivalent electric circuit of the third-evanescent-modes filter.

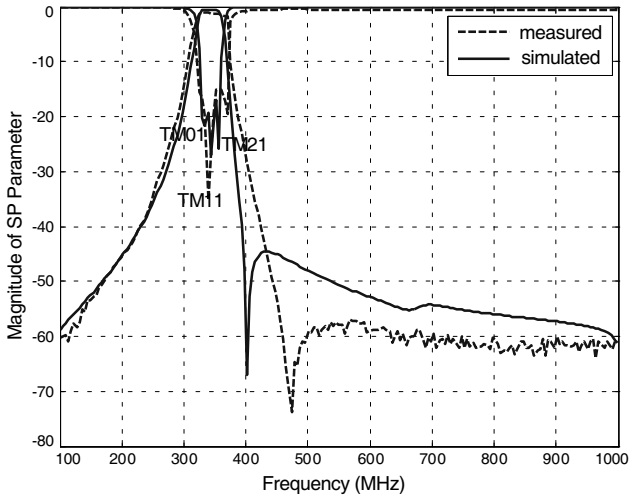


**Figure 9.** The simulated and measured responses of the third-evanescent-modes band-pass filter.

equivalent electric circuit is shown in Fig. 8. The third-order band-pass filter is a combination of three resonant cavities in parallel. A magnetic coupling is used at the exciting ports.

**Table 1.** The parameters for the band-pass filter.

| symbols | $a$ | $b$ | $h$ | $v_r$ |
|---|---|---|---|---|
| value | 23.0 mm | 4.0 mm | 2.5 mm | 0.5 mm |
| symbols | $C_p$ | $C_t$ | $\varepsilon_r$ | $F_L$ |
| value | 42 pF | 3.0 pF | 4.4 | 4.2 mm |

Fig. 9 shows the simulated and measured responses of the third-evanescent-modes band-pass filter. By observing the $S_{11}$, it can be noticed that there are three reflection zeros corresponding to the TM01, TM11 and TM21 modes. The return loss is below $-15$ dB and insertion loss is better than 1.0 dB in the frequency range of 330 MHz to 360 MHz. The out-of-band rejection levels are higher than 45 dB in the frequency range of 450 MHz to 8.0 GHz (and DC to 200 MHz).

## 4. CONCLUSION

A multi-evanescent-mode resonator based on a coaxial cavity is demonstrated in this paper. Due to the combined effects of the evanescent modes and multiple modes, the size of resonator is sufficiently miniature even at UHF band. Considering resonant frequencies and quality factors, TM01, TM11, TM21 modes are suitable to be combined. A third-order band-pass filter is designed based on this resonator, and its characteristics such as low insertion loss, high attenuation in the outband and high selectivity are found excellent. Especially spurious band in about 22 octave-band widths of the central frequency is totally absent.

## ACKNOWLEDGMENT

This work is supported by the Fundamental Research Funds for the Central Universities under the Grant K5051304018, K5051304013 and K5051204003. This work is also supported by the National Key Laboratory Foundation of China under the Grant 9140C530203120C53200.

## REFERENCES

1. Wu, L.-S. and X.-L. Zhou, "A substrate-integrated evanescent-mode waveguide filter with nonresonating node in low-temperature co-fired ceramic," *IEEE Transactions on Microwave Theory and Techniques*, Vol. 58, No. 10, 2654–2662, 2010.
2. Park, S.-J., I. Reines, C. Patel, and G. M. Rebeiz, "High-RF-MEMS 4–6-GHz tunable evanescent-mode cavity filter," *IEEE Transactions on Microwave Theory and Techniques*, Vol. 58, No. 2, 381–389, 2010.
3. Senior, D. E., X. Cheng, and Y.-K. Yoon, "Electrically tunable evanescent mode half-mode substrate-integrated-waveguide resonators," *IEEE Microwave and Wireless Components Letters*, Vol. 22, No. 3, 123–125, 2012.
4. Khalil, D., C. Seassal, and S. Tedjini, "Optical modeling of waveguide photonic nanostructures using the radiation spectrum method (RSM) with evanescent modes," *IEEE Journal*, Vol. 5, No. 1, 127–132, 1999.
5. Rong, Y., K. A. Zaki, and M. Hageman, "Low-temperature cofired ceramic (LTCC) ridge waveguide bandpass chip filters," *IEEE Transactions on Microwave Theory and Techniques*, Vol. 47, No. 12, 2317–2324, 1999.
6. Ludlow, P., V. Fusco, G. Goussetis, and D. E. Zelenchuk, "Applying band-pass filter techniques to the design of small-aperture evanescent-mode waveguide antennas," *IEEE Transactions on Antennas and Propagation*, Vol. 61, No. 1, 134–142, 2013.

7. Liu, X., L. P. B. Katehi, W. J. Chappell, and D. Peroulis, "Power handling of electrostatic MEMS evanescent-mode (EVA) tunable bandpass filters," *IEEE Transactions on Microwave Theory and Techniques*, Vol. 60, No. 2, 270–283, 2012.
8. Moon, S., Sigmarsson, H. Hjalti, H. Joshi, and W. J. Chappell, "Substrate integrated evanescent-mode cavity filter with a 3.5 to 1 tuning ratio," *IEEE Microwave and Wireless Components Letters*, Vol. 20, No. 8, 450–452, 2010.
9. Lin, Y.-F., C.-H. Chen, and K.-Y. Chen, "A miniature dual-mode bandpass filter using Al2O3 substrate," *IEEE Microwave and Wireless Components Letters*, Vol. 17, No. 8, 580–582, 2007.
10. Sun, J, S. and T. Itoh, "Dual-mode tunable filter with simple bandwidth control scheme," *IEEE MTT-S International Microwave Symposium Digest, 2009. MTT'09*, 497–500, Boston, MA, 2009.
11. Amari, S., "Application of representation theory to dual-mode microwave bandpass filters," *IEEE Transactions on Microwave Theory and Techniques*, Vol. 57, No. 2, 430–441, 2009.
12. Shen, W., W.-Y. Yin, and X.-W. Sun, "Compact substrate integrated waveguide (SIW) filter with defected ground structure," *IEEE Microwave and Wireless Components Letters*, Vol. 21, No. 2, 83–85, 2011.
13. Potelon, B. and J.-F. Favennec, "Design of a substrate integrated waveguide (SIW) filter using a novel topology of coupling," *IEEE Microwave and Wireless Components Letters*, Vol. 18, No. 9, 596–598, 2008.
14. Mira, F., J. Mateu, S. Cogollos, and V. E. Boria, "Design of ultra-wideband substrate integrated waveguide (SIW) filters in zigzag topology," *IEEE Microwave and Wireless Components Letters*, Vol. 19, No. 5, 281–283, 2009.
15. Packiaraj, D., M. Ramesh, and A. T. Kalghatgi, "Design of a tri-section folded SIR filter," *IEEE Microwave and Wireless Components Letters*, Vol. 16, No. 5, 317–319, 2006.
16. Ghatak, R., P. Sarkar, R. K. Mishra, and D. R. Poddar, "A compact UWB bandpass filter with embedded SIR as band notch structure," *IEEE Microwave and Wireless Components Letters*, Vol. 21, No. 5, 261–263, 2011.
17. Jeng, Y.-H., S.-F. R. Chang, and H.-K. Lin, "A high stopband-rejection LTCC filter with multiple transmission zeros," *IEEE Transactions on Microwave Theory and Techniques*, Vol. 54, No. 2, Part 1, 633–638, 2006.
18. Piatnitsa, V., E. Jakku, and S. Leppaevuori, "Design of a 2-pole LTCC filter for wireless communications," *IEEE Transactions on Wireless Communications*, Vol. 3, No. 2, 379–381, 2004.
19. Rambabu, K. and J. Bornemann, "Simplified analysis technique for the initial design of LTCC filters with all-capacitive coupling," *IEEE Transactions on Microwave Theory and Techniques*, Vol. 53, No. 5, 1787–1791, 2005.
20. Pozar, D. M., *Microwave Engineering*, 3rd edition, 2011.